*Final Draft*
**of the original manuscript:**

Gomes, D.; Loos, M.R.; Wichmann, M.H.G.; de la Vega, A.; Schulte, K.:
**Sulfonated polyoxadiazole composites containing carbon nanotubes prepared via in situ polymerization**
In: Composites Science and Technology (2008) Elsevier

DOI: 10.1016/j.compscitech.2008.10.008

# Sulfonated polyoxadiazole composites containing carbon nanotubes prepared via in -situ polymerization

*Dominique Gomes*[a,*], *Marcio R. Loos*[a], *Malte H. G. Wichmann*[b], *Alejandra de la Vega*[b] *and Karl Schulte*[b,*]

[a]GKSS Research Center Geesthacht GmbH, Institute of Materials Research, Max Planck Str. 1, D-21502, Geesthacht, Germany

[b]Technische Universität Hamburg-Harburg, Institute of Polymers and Composites, Denickestrasse 15, D-21073 Hamburg, Germany

* Corresponding authors. Tel.: +49 40 7718 3138; fax: +49 40 7718 2002 (K. Schulte).

*E–mail addresses:* mdmdefigueiredogomes@gmx.de (D. Gomes), schulte@tuhh.de (K. Schulte)

ABSTRACT: In the present work, in -situ polymerizations of sulfonated polyoxadiazole through a polycondensation reaction of A-A (hydrazine sulphate) and B-B (aromatic dicarboxylic acid) monomers with carbon nanotubes in poly(phosphoric acid) were performed. The structures of composites were characterized by elemental analysis, Raman and FTIR spectroscopy. The sulfonated polyoxadiazole composites with high molecular weight (in the order of magnitude of $10^5$ g/mol) are soluble in organic solvents and can be cast as dense films. They exhibit good mechanical properties (storage modulus up to around 4 GPa at 300 °C) and an electrical conductivity in the order of $10^{-5}$ S $m^{-1}$. The composites can be used at temperatures as high as 470°C.

*Keywords*: polymers, polyoxadiazole, in -situ polymerization, carbon nanotubes, nanocomposites

## 1. Introduction

The development of high-performance polymers has been a demand from the aerospace industries seeking for new materials. Synthesis of polymers containing oxadiazole rings was part of a NASA program on high performance/high temperature polymer for potential use as coatings and composite matrices on aerospace vehicles [1,2]. Particularly, polyoxadiazole (POD) thermoplastic polymers have a great potential as structural material because of their superior thermal, chemical and mechanical properties [3]. POD fibers present a combination of properties (such as good strength and stiffness, good fatigue resistance and low density) that makes these fibers competitive in performance when compared to other reinforcing agents, such as glass, steel, and commercial high-temperature fibers (Kevlar, X-500, Cermel, Nomex) [3-5]. Technological applications have also been reported in connection with the basic nitrogen atoms and aromatic character of the oxadiazole heterocyclic ring [6], enabling their use as emissive layers in light-emitting diodes [7-9], electron/proton conducting materials [10,11], electrochemical/acid sensors [12,13] and materials to prevent metal corrosion [14,15].

During the last decade, composite materials have become commonplace in space structures. Recent applications of fiber -reinforced polymers in aircraft propulsion systems have resulted in substantial reductions in both engine weight and manufacturing costs [16,17]. A major effort underway in this area is the development of high-temperature fiber -reinforced polymers, usable up to temperatures as high as 425°C [18,19]. Continued improvements in the stability of polymer matrices coupled with improvements in polymer/filler interfaces, composite processing, and oxidation-resistant coatings will yield reinforced polymers for use at high temperatures [18,20,21].

Incorporation of carbon nanotubes (CNTs) into polymeric materials has been the subject of growing interest because the individual properties of the two or more materials can be

combined to give a composite with improved mechanical, electrical, thermal and/or optical properties [22-26]. However, the use of CNTs presents challenges to be overcome as with nanoparticles in general. The particle size, volume content and surface properties of CNTs, influences the degree of dispersion and interfacial adhesion. Various physical, chemical, or combined approaches have been reported to afford homogeneous dispersion of fillers in the polymeric matrix [26-32]. Baek et al. [28] described functionalization of Vapor-Grown Carbon Nanofibers (VGCNF) by a in -situ *meta*-poly(ether-ketone) (PEK) polymerization of an AB monomer via a direct Friedel-Crafts arylcarbonylation in poly(phosphoric acid) (PPA) at 130°C for 51h. A uniform grafting of linear polymer onto VGCNF has been achieved. Oh et al. [27] described a grafting of polyetherketone onto Multi-Walled Carbon Nanotube (MWCNT) and VGCNF by in -situ polycondensation of the AB monomers, 3- and 4-phenoxybenzoic acids in viscous PPA at 130°C for 48h. Evidences have been shown that both MWCNT and VGCNF remained structurally intact during the in situ polymerization [27]. Recently, Wang et al. [29] showed that hyperbranched PEK-VGCNFs synthesized in PPA at 130°C for 51h have considerably better solubility (e.g., in aprotic polar solvents) than their linear analogues described by Baek et al. [28]. Greatly reduced viscosities for the hyperbranched polymers were obtained.

Though VGCNFs are very attractive compared to CNTs because of their relative low cost and availability in larger scale [28,29], their larger diameter (60-200 nm) compared to SWCNTs (1-2 nm) and the MWCNts (13-16 nm) should make the covalent sidewall functionalization with polyoxadiazole chains more difficult. VGCNFs are structurally hollow and multiwalled with length in the range of 50-100 μm and an aspect ratio (a= length/diameter) greater than 800 [28,29]. The high specific surface area (SSA) of CNTs as well as the aspect ratio are dependent on the diameter and the number of sidewalls [23]. The surface area of nanotubes can act as desirable interface for stress transfer, but undesirably induces strong attractive forces between the CNTs themselves, leading to excessive

agglomeration behavior. This way, SWCNTs with the largest aspect ratio and SSA up to 1300 $m^2/g$ should present higher reinforcing potential compared to the MWCNTs (SSA of only 200 $m^2/g$ or less) [23]. On the other hand, MWCNTs exhibit much better dispersibility which may improve the mechanical properties. As an improvement of the CNT dispersibility should already be achieved in the present work by polyoxadiazole/CNT functionalizations and taking into account the lower diameter of the SWCNTs, for this study SWCNTs were selected and tested in a wider range of concentration (0.1-15 wt.%). For the sake of comparison, polyoxadiazole-based composites containing 1wt.% and 10wt.% MWCNT were also analyzed.

The present work relates to a fast direct method where the CNTs are in -situ functionalized during the polyoxadiazole polymerization. Because of the different reactivity of monomers, significant lower synthesis time is required (4h) to produce the composite polyoxadiazole compared to other composite polymers synthesized via in -situ polymerization in PPA [27-29]. The sulfonated polyoxadiazole composites with high molecular weight (in the order of magnitude of $10^5$ g/mol) are soluble in organic solvents and can be cast as dense films. They exhibit good mechanical properties (storage modulus up to around 4 GPa at 300 °C) and an electrical conductivity in the order of $10^{-5}$ S $m^{-1}$.

## 2. Experimental Section

### *2.1. Synthesis of sulfonated poly(diphenyether-1,3,4-oxadiazole) nanocomposites*

The synthesis conditions have been selected considering a previously reported synthesis method for sulfonated polyoxadiazoles with high molecular weight [33,34]. Hydrazine sulfate salt, HS (>99%, Aldrich), carbon nanotubes, CNT, and dicarboxylic diacid 4,4'-diphenylether, DPE (99%, Aldrich) were reacted at 160°C in polyphosphoric acid, PPA (115% $H_3PO_4$, Aldrich), under dry nitrogen atmosphere for 4 h. The multi-wall carbon nanotubes, MWCNTs (>95%, average outer diameter: 13-16 nm, length 1-10 μm) were kindly

supplied by Bayer MaterialScience and the single-wall carbon nanotubes, SWCNTs (>95%, average outer diameter: 1-2 nm, length 10-20 μm) were purchased from Heji Inc..

The molar dilution rate (PPA/HS) and the molar monomer rate (HS/DPE) were kept constant and equal to 10 and 1.2, respectively. Afterwards, the reaction medium was poured into water containing 5 wt.% of sodium hydroxide (99%, Vetec), for precipitation of the polymer composites. The pH of this polymer suspension was controlled according to literature [34]. Yield: 97-99%.

Homogeneous films were cast from solutions with a polymer concentration of 4 wt. % in dimethyl sulfoxide, DMSO (>99%, Aldrich). After casting, the DMSO was evaporated in a vacuum oven at 60°C for 24 h. For further residual solvent removal, the films were immersed in a water bath at 60°C for 48 h and dried in a vacuum oven at 60°C for 24h. The final thickness of the films was about 70 μm.

*2.2. Polymer and nanocomposite characterization*

The polymer and nanocomposite structures were characterized by elemental analysis, Raman and infrared spectroscopy. Elemental analysis was conducted on a Carlo Erba Elemental Analyzer-Mod 1108. Raman spectra were recorded on a Jobin Yvon HR800 LabRam spectrometer, using the 633 nm laser line. Infrared spectra were recorded on a Bruker Equinox IFS 55 spectrophotometer in the range 4000-400 $cm^{-1}$, using film samples. A Viscotek SEC apparatus equipped with Eurogel columns SEC 10.000 and PSS Gram 100, 1000, with serial numbers HC286 and 1515161 and size 8 x 300 mm was employed to evaluate the weight average molecular weights of polymer and nanocomposite samples. The equipment was calibrated using polystyrene standards (Merck) with weight average molecular weights ranging from 309 to 944,000 g/mol. A solution with 0.05 M lithium bromide in dimethylacetamide, DMAc (≥99.9%, Aldrich) was used as the carrier. Solutions with 0.5

wt.% of the composite polyoxadiazoles were prepared, filtered through 0.2 μm and injected into the chromatograph.

The film morphology was observed by Scanning Electron Microscopy (SEM) type LEO 1550VP. The samples were previously coated with gold in a sputtering device.

Thermogravimetric analysis (TGA) experiments were carried out in a Netzsch 209 TG, equipped with a TASC 414/3 thermal analysis controller. The bulk sample, under nitrogen atmosphere, was heated from 100°C to 700°C at 10°C/min. Dynamic Mechanical Thermal Analysis (DMTA) was used for determination of the glass transition temperature ($T_g$), storage modulus (E'), loss modulus (E'') and loss tangent (Tan δ). DMTA was performed using a TA instrument RSA 2 with a film tension mode at a frequency of 1Hz and 0.1 N initial static force. The temperature was varied from 25°C to 500 °C at a heating rate of 2°C/min and at a constant strain of 0.05%.

The electrical conductivity was measured by dielectric spectroscopy using a HP 4284a impedance analyzer. The samples (each three specimens) were tested with a voltage amplitude of 1.0 V in a frequency range between 20 Hz and 1MHz. The samples were coated with a thin silver film acting as electrodes. The values obtained for 100 Hz were chosen for comparison of the polyoxadiazole nanocomposites containing 0.1 to 15 wt.% SWCNT.

## 3. Results and Discussion

### *3.1. Synthesis and characterization of sulfonated polyoxadiazole composites containing carbon nanotubes*

Sulfonated polyoxadiazole composites containing carbon nanotubes were prepared via in-situ polymerization as schematically shown in figure 1. The differences in the color for the pristine sulfonated polyoxadiazole and composites are presented in this figure. Proposed non-covalent and covalent polyoxadiazole/CNT functionalizations are also shown in this Figure.

The non covalent functionalizations are represented by the protonation of the basic nitrogen atoms ($NH^+$) by acid groups (COOH) as well as by the interaction between aromatic groups from the diphenyl ether group with the CNTs, which is based on the ability of the extended $\pi$-system of the carbon nanotubes sidewall to bind guest molecules via $\pi$-$\pi$-stacking interactions. Covalent attachment of POD onto the CNT surfaces should be expected to occur both by Friedel-Craft acylation between C=O groups of the acid momomer and C=C of the CNTs [27], as well as condensation reaction of in-situ COOH groups generated on the surface of the CNTs with the $NH_2NH_2$ hydrazine monomer, leading to the formation of arylcarbonyl and $CONHNH_2$, respectively. Formation of hydrazide groups (CONHNHCO) is expected based on the reaction between $CONHNH_2$ and C=O groups of the acid momomer.

The polyoxadiazole synthesis described here follows the classical mechanism of polymerization by polycondensation [35]. In this case, the polymerization takes place by the continuous reaction between the functional groups of the multi-functional molecules. The basic characteristics of these reactions are known since the beginning of the 20's century [36] and include the continuous growth of the average molecular weight with time, the high sensitivity to mono-functional impurities and the possibility of the formation of three-dimensional crosslinked structures, when there is presence of three or more reactive groups per molecule. Against what could be expected, taking into account that polycondensation reactions could be draw backed in the presence of CNTs, which could act as an "impurity", sulfonated polyoxadiazole composites containing carbon nanotubes were successfully prepared via in- situ polymerization, as observed as follows by elemental analysis, FTIR and Raman spectra.

Elemental analysis data for the sulfonated polyoxadiazole nanocomposites shown in Table 1 are in agreement with the value range for the sulfonated polyoxadiazoles. The polyoxadiazole sulfonation reaction which occurs during this synthesis method by the presence of sulfuric acid in the solution of hydrazine sulfate has been recently recognized and characterized by

Gomes et al. [10]. The polyoxadiazole sulfonation level (S/C) has been shown to be dependent on the reaction time [11], reaching the value range 0.098-0.085 for the synthesis performed in 4 h. Here, the sulfonation level has been mainly changed for the higher CNT contents (Table 1). In the range of concentration 0.1 to 5 wt.% the differences are most within the ones observed for the sulfonated polyoxadiazoles. An additional factor could be the homogeneity differences of CNT concentration in the reaction medium. In regions where the CNT concentration is overall or much better distributed, the sulfonation level should proportionally decrease. This explains the lower sulfonation level obtained for the concentrations 10 and 15 wt.% CNT.

The comparison of the composites with the pristine sulfonated polyoxadiazole is difficult once the polymer shows different sulfonation levels (S/C), which influence the dipole-dipole interactions between the sulfonated groups. The introduction of sulfonic acid groups increases the intermolecular interaction and consequently increasing the $T_g$ and mechanical properties. Despite of that, an increase in mechanical properties has been observed for both systems. In the range of concentration 0.2 to 5 wt.% CNT sulfonation level did not change very much compared to the value range for the pristine polymer, therefore the observed changes in the storage modulus can be attributed to the CNT homogeneity differences within the polymer matrix. For the lower concentration 0.1 wt.% SWCNT, the CNTs should be better distributed, which explains the high storage modulus despite the lower sulfonation level. The decrease of the storage modulus with increase of 5 wt.% to 15 wt.% SWCNT can be both attributed to the lower sulfonation level as well to the lower CNT homogeneity within the polymer matrix when CNT concentration increases. High storage modulus values up to 3.6 GPa at 300 $^{o}$C have been obtained for composite films containing 10 wt.% MWCNT and 5 wt.% SWCNT with similar $T_g$ (tan δ) around 430 °C. A deeper explanation about the effect of sulfonation level and CNT content on the $T_g$ of the composites will be discussed in section 3.3. These composites exhibit 44% increment in the storage modulus compared with the pristine

sulfonated polyoxadiazole. Liu et al. [37] have also obtained 43% increment in the storage modulus of MWCNT/Polyamide composites compared with the pristine polymer. The significant improvement in the storage modulus can be attributed to the high performance and well dispersion of CNTs in the sulfonated polyoxadiazole matrix.

High molecular weights in the order of magnitude of $10^5$ g/mol with a polydispersity around 2 for the MWCNT-based composites were obtained (Table 2). Composites prepared with SWCNTs were not soluble in DMAc, therefore their molecular weights could not be measured. The difference in solubility of both composites can also be attributed to the different CNT reactivities.

Thermal degradation behavior of composites containing MWCNTs and SWCNTs was analyzed by TGA and the results are shown in Tables 2 and 3, respectively. SWCNT-based composites show 5% weight loss ($T_{d5}$) in the range of 465-472$^o$C with residue at 700$^o$C in the range of 57-63%, exhibiting better thermal stability than those prepared with MWCNTs. This result maybe attributed to the higher SWCNT dispersion and better polymer wetting due to the higher SWCNT reactivity.

Attempts to confirm the covalent attachment shown in Figure 1were done by analyzing the FTIR and Raman spectra of the composites. Figure 2 shows representative FTIR spectra of pristine sulfonated polyoxadiazole (POD) and of the composite (PODCNT). No difference could be observed for the different CNT compositions. The analysis of this figure indicates that no additional band and no shifted band can be detected for the composite. Qualitatively, the intensity band of the asymmetric $SO_2$ stretch at 1396 $cm^{-1}$ relative to C=C stretching of the aromatic groups decreased, indicating that sample is less sulfonated than the pristine polymer [10], as already observed by elemental analysis results. Other assignments for the pristine polymer at 1602 and 1485 $cm^{-1}$ arising from C=C stretching of the aromatic groups, the assignments placed at 1468 $cm^{-1}$ and 1417 $cm^{-1}$ related to the C=N stretching of oxadiazole ring group [38]. In Figure 3 are shown Raman spectra of SWCNT and of sulfonated

polyoxadiazole nanocomposites containing 0.1-15 wt.% SWCNT. As shown in Figure 3, all composites show similar bands present in the pristine sulfonated polyoxadiazole at 1618 $cm^{-1}$, 1560 $cm^{-1}$ and 1425 $cm^{-1}$ attributed to the aromatic groups and at 1167 $cm^{-1}$ relative to sulphonated groups of the main chain of the polyoxadiazole [35]. Bands at 1497 $cm^{-1}$ and at 1001 $cm^{-1}$ due to the oxadiazole ring are also observed. The D- and G-bands of SWCNTs at 1331 $cm^{-1}$ and 1594 $cm^{-1}$, attributed respectively to the disorder and graphite modes, are observed only for the composites containing 5 and 15 wt.% SWCNT. Second-order D* band of SWCNTs appears in both systems at 2642 $cm^{-1}$. For composites containing 0.1 to 1 wt.% SWCNT, the signals of the polymer overcomes completely that of the nanotubes. This is most likely because when the amount of SWCNTs is too low, the nanotubes should be completely wrapped by the polymer chains. Unfortunately, no C=O stretches could be observed both by the FTIR and Raman spectra of the composites. This result may be attributed to the very low surface amount of C=O groups compared with the other groups present in the main polymer chain.

*3.2. Morphological properties*

Figures 4 and 5 show the typical SEM images of SWCNT and MWCNT as well as their composites. The MWCNTs shown in Fig. 4(a) have an entangled cotton-like structure, whereas the SWCNTs are a more condensed and highly entangled network structure (Fig. 5(a)). The micrographs show uniform distribution of CNTs in the sulfonated polyoxadiazole matrix, indicating that the CNTs are well dispersed in the composite. However, the morphology of the bulk composites is different for both CNTs. For the sulfonated polyoxadiazole with 1 and 10 wt.% MWCNTs, there are more than expected exposed MWCNTs taking into account the range of composition (Fig. 4 (b-c)). The CNT bundles are probably pulled out of the sulfonated polyoxadiazole matrix. On the other hand, for sulfonated polyoxadiazole with 0.2 and 15 wt.% SWCNTs (Fig. 5 (b-c)), a higher CNT dispersion and

better polymer wetting is observed. For the composite containing 15 wt.%, because of the higher concentration, SWCNTs wrapped by the sulfonated polyoxadiazole matrix are also observed. The difference observed for both CNTs can be attributed to the higher reactivity of SWCNTs and therefore better CNT functionalization with the polymeric matrix, which again explains the higher thermal stability of the SWCNT composites than those prepared with MWCNTs. On the other hand for the composite films no agglomerates and any difference could be observed with increase of CNT concentration for both CNTs. The composite films prepared with 1 wt.% MWCNTs and SWCNTs have similar structures as shown in Figures 4 (d) and 5 (d), respectively. The observed bright dots are attributed to protruding CNTs as well as bow-type CNTs with their middle part up way from the polymeric matrix [39-40].

### *3.3. Glass transition temperatures of sulfonated polyoxadiazole composites containing carbon nanotubes*

The $T_g$ values of the composites are affected both by the sulfonation level as well as by the CNT content (Fig. 6). The higher the sulfonation level, the higher is the $T_g$ [11]. When a filler is homogeneously distributed in a polymeric matrix, the $T_g$ of the composites should increase with filler content. The $T_g$ values of the composites in general slightly decreased or kept unchanged with the addition of CNTs, excepted for 1 wt.% CNT. For this composition, where the sulfonation level is similar to the pristine polymer, the effect of the addition of CNTs should be predominant for the final $T_g$ value. On the other hand, despite the addition of 15 wt.% CNT, a reduction in $T_g$ was observed because the sulfonation level also significantly decreased.

High interactions between the CNTs and the polyoxadiazole result in constrained polymer chains in the vicinity of the CNTs. This effect was observed by the depression in tan δ, which indicates the reduction of chain mobility during the glass transition being the relative peak height proportional to the volume of the constrained chains [41]. Fig. 6 clearly shows the

reduction of the relative peak height of tan δ and the decrease of the $T_g$ value for the composite containing 15 wt.% CNT, which indicate a very well dispersion of CNTs in the sulfonated polyoxadiazole matrix. Reductions of the relative peak height of tan δ with the increase of the $T_g$ values due to the constrained polymer chains in the vicinity of the functionalized filler were also observed by Gomes et al. [42].

Figure 7 shows the dependence of the $T_g$ on the sulfonation level (S/C) of the sulfonated polyoxadiazole composites. As already expected, the higher the sulfonation level, the higher is the $T_g$. The observed deviation can be attributed to the effect of CNT addition, which is affected both by the CNT amount and dispersion. Recently, Gomes et al. [42] have shown that when functionalized nanofiller is added to the sulfonated polyoxadiazole matrix which was synthesized in a different batch, the $T_g$ values of the composite membranes increased with increase of nanofiller concentration as a consequence of the good interaction between the functionalized filler and the polyoxadiazole matrix. When the filler had a good interaction with the polyoxadiazole matrix, for a constant S/C the $T_g$ increased and the relative peak height decreased. Gomes et al. [42] have also shown that for a concentration range 2.5-5wt.% of a nanofiller, fluctuations in the filler dispersion in the sulfonated polyoxadiazole matrix lead to not significant differences in the $T_g$ values for this concentration range.

### *3.4. Electrical conductivity*

Fig. 8 shows the electrical conductivity values of the SWCNT-based polyoxadiazole nanocomposites at 100 Hz. The insert in this figure shows the conductivity plotted as a function of frequency for the different SWCNT concentrations. At concentration levels below 15 wt.%, a strong frequency dependence of the conductivity is observed. However, a typical dielectric behavior is not observed for the samples with low SWCNT concentration, which should exhibit a linear increase of conductivity with frequency with a slope of unity in a log-log scale. Musumeci et al. [43] have argued that conjugated polymers behave different from

insulating polymers and that for composites with low CNT concentration, the conductivity is associated with charge transfer through the semiconductor polymer. The polymer layer between CNT connections presents a resistance for the electrical pathway. Conjugated polymer based nanocomposites have presented lower levels of conductivity than insulating polymers after percolation [45]. A combination of CNT network conductivity and conjugated polymer charge transport should play different roles for different CNT concentrations. Reduction of polymer thickness could be a possible way to increase composite conductivity by introducing the tunneling mechanism of conduction [32,45]. Another possibility to increase the composite conductivity should be the doped form of basic polymers [32]. Though with 1 wt. % a high electrical conductivity up to 2.7 $x10^{-5}$ S $m^{-1}$ has already been achieved, only the composite with 15 wt.% concentration exhibited a conductive behavior, where the conductivity is nearly independent of frequency. As it can be seen in Fig. 9, the sulfonated polyoxadiazole is a semiconductor material with an electrical conductivity of 2.3 $x10^{-7}$ S $m^{-1}$, higher than insulating polymers with the order of magnitude in the range $10^{-16}$-$10^{-8}$ S $m^{-1}$ [24,32,44]. The semiconductor behavior of the sulfonated polyoxadiazole samples is a consequence of the conjugated and aromatic character of the polyoxadiazole chains as well as of the sulfonation level once the introduction of sulfonic acid groups and the consequent presence of mobile metal counter-ions might make ease the electron transport [46]. Therefore, the electrical conductivity values plotted in Fig. 8 may depend not only on the content of SWCNTs in the composite but also on the content of sulfonic acid groups acting as a self doping agent.

## 4. Conclusions

In-situ polymerizations of sulfonated polyoxadiazole through a polycondensation reaction of A-A (hydrazine sulphate) and B-B (aromatic dicarboxylic acid) monomers with carbon nanotubes (CNTs) in poly(phosphoric acid) were successfully performed in 4 h, as confirmed

by elemental analysis, FTIR and Raman spectra. High storage modulus values up to 3.6 GPa at 300 $^{o}$C were obtained for composite films with similar $T_g$ (tan δ around 430 °C) of the pristine sulfonated polyoxadiazole, exhibiting 44% increment compared with the polymer. SEM images show a uniform distribution of CNTs in the sulfonated polyoxadiazole matrix, indicating that the CNTs are well dispersed in the composites. The $T_g$ values of the composites are affected both by the sulfonation level as well as by the CNT content. The composites show electrical conductivity in the order of magnitude $10^{-5}$ S $m^{-1}$, indicating that they can be used as antistatic materials and at temperatures as high as 470°C.

**Acknowledgments.** The authors thank the Helmholtz-University Junior Group Project (VH-NG-323) for supporting this research and H. Böttcher for the DMTA measurements.

**References**

[1] Hergenrother P M, Jensen B J, Havens S J. Poly(arylene ethers). Polymer 1988; 29:358-369.

[2] Cornell J W, Hergenrother PM, Wolf P. Chemistry and properties of poly(arylene ether 1,3,4-oxadiazole)s and poly(arylene ether 1,2,4-triazole)s. Polymer 1992; 33:3507-3511.

[3] Nanjan M J. Encyclopedia of Polymer Science and Engineering. New York: Wiley, 1987.

[4] Yang H H. Aromatic High-Strength Fibers. New York: Wiley, 1989.

[5] Bach HC, Dobinson F, Lea KR, Saunders JH. High-strength/high-modulus fibers of p-phenylene oxadiazole/n-methyl hydrazide copolymers - a new class of high-performance organic materials. J. Appl. Polym. Sci. 1979;23:2125-2131.

[6] Cotter RJ, Matzner M, Ring-Forming Polymerizations. In: Blomquist AF., Wasserman, H, editors. Heterocyclic Rings, 13B, Part B1, New York: Academic Press, 1972.

[7] Liou G S, Hsiao S H, Chen WC, Yen H J. A new class of high *t*g and organosoluble aromatic poly(amine-1,3,4-oxadiazole)s containing donor and acceptor moieties for blue-light-emitting materials. Macromolecules 2006;39:6036-6045.

[8] Kulkarni A P, Tonzola C J, Babel A, Jenekhe S A. Electron transport materials for organic light-emitting diodes. Chem. Mater. 2004;16:4556-4573.

[9] Janietz S, Anlauf S, Macromol. A new class of organosoluble rigid-rod, fully aromatic poly(1,3,4-oxadiazole)s and their solid-state properties, 2[a] solid-state properties. Macromol. Chem. Phys 2002;203:427-432.

[10] Gomes D, Roeder J, Ponce M L, Nunes S P. Characterization of partially sulfonated polyoxadiazoles and oxadiazole–triazole copolymers. Journal of Membrane Science 2007;295:121-129.

[11] Gomes D, Roeder J, Ponce M L, Nunes S P. Single-step synthesis of sulfonated polyoxadiazoles and their use as proton conducting membranes. Journal of Power Sources 2008;175:49-59.

[12] Wu T Y, Sheu R B, Chen Y. Synthesis and optically acid-sensory and electrochemical properties of novel polyoxadiazole derivatives. Macromolecules 2004;37 :725-733.

[13] Yanga N C, Changb S, Suh D H. Synthesis and optically acid-sensory properties of novel polyoxadiazole derivatives. Polymer 2003;44:2143-2148

[14] Kannan B, Gomes D, Dietzel W, Abetz V, Polyoxadiazole-based coating for corrosion protection of magnesium alloy. Surface and Coatings Technology 2008; doi:10.1016/j.surfcoat.2008.03.027.

[15] Lagrenee M, Mernari B, Chaibi N, Traisnel M, Vezin H, Bentiss F. Investigation of the inhibitive effect of substituted oxadiazoles on the corrosion of mild steel in HCl medium. Corrosion Sci. 2001;43:951-962.

[16] Soutis C. Carbon fiber reinforced plastics in aircraft construction. Materials Science and Engineering A 2005;412:171–176.

[17] Meador M A, Campbell S G, Chuang K C, Scheimann D A, Mintz E, Hylton D, Veazie D, Criss J, Kollmansberg R, Tsotsis T. Low-cost, High temperature polymeric materials for space transportation propulsion applications. NASA Technical Reports Server NTRS 2004; Document ID: 20040020118.

[18] http://www.key-to-metals.com/Article103.htm.

[19] Chuang K C. Low-cost, high glass-transition temperature, thermosetting polyimide developed. NASA Technical Reports Server NTRS 2006; Document ID: 20050187016.

[20] Wilson D. Polyimide matrix composites: candidates for high speed commercial aircraft or not? High Performance Polymers 1991;3:73-87.

[21] Miller S, Papadopoulos D, Heimann P, Inghram L, McCorkle L. Graphite sheet coating for improved thermal oxidative stability of carbon fiber reinforced/PMR-15 composites. Composites Science and Technology 2007;66:2183–2190.

[22] Ajayan M, Tour J M. Nanotubes composites. Nature 2007;447:1066-1068.

[23] Gojny F H, Wichmann M H G, Fiedler B, Schulte K. Influence of different carbon nanotubes on the mechanical properties of epoxy matrix composites – A comparative study. Composites Science and Technology 2005;65:2300-2313.

[24] Gojny F H, Wichmann M H G, Fiedler B, Bauhofer W, Schulte K. Influence of nano-modification on the mechanical and electrical properties of conventional fibre-reinforced composites. Composites Part A: Applied Science and Manufacturing 2005;36:1525-1535.

[25] Gojny F H, Wichmann M H G, Fiedler B, Kinloch I A, Bauhofer W, Windle A H, Schulte K. Evaluation and identification of electrical and thermal conduction mechanisms in carno nanotubes/epoxy composites. Polymer 2006;47:2036-2045.

[26] Smith J G, Connell J W, Deloziera D M, Lilleheia P T, Watsonb K A, Linc Y, Zhouc B, Sunc Y P. Space durable polymer/carbon nanotube films for electrostatic charge mitigation. Polymer 2004;45:825-836.

[27] Oh S J, Lee H J, Keum D K, Lee S W, Wang D H, Park S Y, Tan L S, Baek J B. Multiwalled carbon nanotubes and nanofibers grafted with polyetherketones in mild and viscous polymeric acid. Polymer 2006;47:1132-1140.

[28] Baek J B, Lyons C B, Tan L S. Grafting of vapor-grown carbon nanofibers via in-situ polycondensation of 3-phenoxybenzoic acid in poly(phosphoric acid). Macromolecules 2004;37:8278-8285.

[29] Wang D H, Mirau P, Li B, Li C Y, Baek J B, Tan L S. Solubilization of carbon nanofibers with a covalently attached hyperbranched poly(ether ketone). Chem. Mater. 2008;20:1502-1515.

[30] Kuan H C , Ma C C M, Chang W P, Yuen S M, Wu H H, Lee T M, Synthesis, thermal and rheological properties of multiwall carbon nanotubes/waterbone polyurethane nanocomposite. Composites Science and Technology 2005;65:1703-1710.

[31] Singh K V, Pandey R R, Wang X, Lake R, Ozkan C S, Wang K, Ozkan M. Covalent functionalization of single walled carbon nanotubes with peptide nucleic acid: Nanocomponents for molecular level electronics. Carbon 2006;44:1730-1739.

[32] Konyushenko E N, Stejskal J, Trchová M, Hradil J, Kovářová J, Prokeš J, Cieslar M, Hwang J Y, Chen K H, Sapurina I. Multi-wall carbon nanotubes coated with polyaniline Polymer 2006;47: 5715-5723.

[33] Gomes D, Borges C P, Pinto J C. Study of the synthesis of poly(4,4'-diphenylether-1,3,4-oxadiazole) in solutions of poly(phosphoric acid). Polymer 2001;42:851-865.

[34] Gomes D, Borges C P, Pinto J C. Effects of reaction variables on the reproducibility of the syntheses of poly-1,3,4-oxadiazole, Polymer 2004;45:4997-5004.

[35] Odian G, Principles of Polymerization, New York, John Wiley&Sons,1991.

[36] Flory P J, Principles of Polymer Chemistry, New York, Cornell University Press, 1953.

[37] Liu T, Phang I Y, Shen L, Chow S Y, Zhang W. Morphology and mechanical properties of multiwalled carbon nanotubes reinforced nylon-6 composites. Macromolecules 2004;37:7214-7222.

[38] G. Socrates, Infrared and Raman Characteristic Group Frequencies Tables and Charts Chichester: John Wiley & Sons, 2001.

[39] Lim J K, Yun W S, Yoon M, Lee S K, Kim C H, Kim K, Kim S K. Selective thiolation of single-walled carbon nanotubes. Synthetic Metals 2003;139:521-527.

[40] Phang I Y, Liu T, Zhang W, Schönherr H, Vancso G J. Probing buried carbon nanotubes within polymer-nanotube composite matrices by atomic force microscopy. European Polymer Journal 2007;43:4136-4142.

[41] Rao Y, Pochan J M. Mechanics of Polymer-clay nanocomposites, Macromolecules 2007;40: 290-296.

[42] Gomes D, Marschall R, Nunes S P, Wark M. Development of Polyoxadiazole Nanocomposites for High Temperature Polymer Electrolyte Membrane Fuel Cells. *J. Membr. Sci.* 2008;322:406-415.

[43] Musumeci A W, Silca G G, Liu J W, Martens W N, Waclawik E R. Structure and conductivity of multi-walled carbon/poly(3-hexylthiphene) composite films. Polymer 2007;48:1667-1678.

[44] Ounaies Z, Park C, Wise K E, Siochi E J. Electrical properties of single wall carbon nanotubes reinforced polyimide composites. Composites Science and Technology 2003;63:1637-1646.

[45] Kilbride B E, Coleman J N, Fraysse J, Fournet P, Cadek M, Drury A, Hutzler S, Roth S, Blau W J. Experimental observation of scaling laws for alternating current and direct

current conductivity in polymer-carbon nanotube composite thin films. Journal of Applied Physics 2002;92:4024-4030.

[46] Meerholz K. Enlightening solutions. Nature 2005;437:327-328.

Tables

**Table 1.** Elemental analysis data and empirical formulas for the sulfonated polyoxadiazole nanocomposites.

**Table 2.** Structural, thermal and mechanical properties of sulfonated polyoxadiazole nanocomposites containing 1 and 10 wt.% MWCNT.

**Table 3.** Structural, thermal and mechanical properties of sulfonated polyoxadiazole nanocomposites containing 0.1-15 wt. % SWCNT.

**Figure Captions**

**Figure 1.** In -situ polymerization of AA and BB monomers with CNT.

**Figure 2.** Representative FTIR spectra of pristine sulfonated polyoxadiazole (POD) and of the composite (PODCNT).

**Figure 3.** Raman spectra of SWCNT and of sulfonated polyoxadiazole nanocomposites containing 0.1-15 wt. % SWCNT.

**Figure 4.** SEM micrographs of the MWCNTs (a) and of the cross-section of the bulk sulfonated polyoxadiazole nanocomposite containing 1 wt.% MWCNT (b) and 10 wt.% MWCNT (c) and of the sulfonated polyoxadiazole nanocomposite film containing 1 wt.% MWCNT (d).

**Figure 5.** SEM micrographs of the SWCNTs (a) and of the cross-section of the bulk sulfonated polyoxadiazole nanocomposite containing 0.2 wt.% SWCNT (b) and 15 wt.% MWCNT (c) and of the sulfonated polyoxadiazole nanocomposite film containing 1 wt.% MWCNT (d).

**Figure 6.** Trace of tan δ vs temperature as measured by DMTA at 1 Hz for the nanocomposites containing 0.1-15 wt.% SWCNT.

**Figure 7.** S/C versus $T_g$ of the sulfonated polyoxadiazole composites.

**Figure 8.** Electrical conductivity values of the SWCNT-based polyoxadiazole nanocomposites.

| CNT (wt.%) | S/C | | Elemental Analysis C (%) | N (%) | S (%) | Empirical Formula |
|---|---|---|---|---|---|---|
| | Calcd. | found | | | | |
| **0** | 0 | | 71.2 | 11.9 | 0 | $[(C_{14}H_8N_2O_2)]$ (236) |
| **0** | 0.099 | 0.098-0.085 | 48.6 | 8.14 | 4.74 | $[(C_{14}H_8N_2O_2)_{0.48}.(C_{14}H_8N_2O_5SNa)_{0.52}]$ (289) |
| **SWCNT** | | | | | | |
| **0.1** | 0.099 | 0.075 | 54.7 | 9.37 | 4.08 | $[(C_{13.99}H_8N_2O_2)_{0.605}.(C_{13.99}H_8N_2O_5SNa)_{0.395}]$ (276) |
| **0.2** | 0.099 | 0.087 | 53.5 | 9.21 | 4.63 | $[(C_{13.98}H_8N_2O_2)_{0.542}.(C_{13.98}H_8N_2O_5SNa)_{0.458}]$ (282) |
| **0.5** | 0.099 | 0.081 | 56.8 | 9.58 | 4.62 | $[(C_{13.94}H_8N_2O_2)_{0.574}.(C_{13.94}H_8N_2O_5SNa)_{0.426}]$ (278) |
| **1** | 0.099 | 0.091 | 55.7 | 9.45 | 5.07 | $[(C_{13.88}H_8N_2O_2)_{0.521}.(C_{13.88}H_8N_2O_5SNa)_{0.479}]$ (282) |
| **5** | 0.098 | 0.081 | 55.3 | 8.87 | 4.46 | $[(C_{13.4}H_8N_2O_2)_{0.542}.(C_{13.4}H_8N_2O_5SNa)_{0.458}]$ (267) |
| **15** | 0.097 | 0.059 | 60.6 | 8.78 | 3.57 | $[(C_{13.2}H_8N_2O_2)_{0.542}.(C_{13.2}H_8N_2O_5SNa)_{0.458}]$ (231) |
| **MWCNT** | | | | | | |
| **1** | 0.099 | 0.092 | 54.1 | 9.03 | 4.99 | $[(C_{13.99}H_8N_2O_2)_{0.516}.(C_{13.99}H_8N_2O_5SNa)_{0.484}]$ (267) |
| **10** | 0.098 | 0.049 | 54.4 | 8.42 | 2.64 | $[(C_{12.8}H_8N_2O_2)_{0.742}.(C_{12.8}H_8N_2O_5SNa)_{0.258}]$ (243) |

(Table 1)

| Polymer Sample | $T_g$ (°C) [a] | | $T_{d5}$ | Residue | $M_w$ | D [e] | S/C [f] | Storage modulus (GPa) | |
|---|---|---|---|---|---|---|---|---|---|
| + MWCNT | E'' | Tan δ | (°C) [b] | (%) [c] | (g/mol) [d] | | | at 100 °C | at 300 °C |
| - | 415 | 429 | 465 | 65 | 330 000 | 2.3 | 0.098-0.085 | 4.1 | 2.5 |
| 1 wt. % | 419 | 434 | 450 | 52 | 420 000 | 2.1 | 0.092 | 4.5 | 3.1 |
| 10 wt. % | 409 | 432 | 451 | 61 | 300 000 | 1.7 | 0.049 | 4.2 | 3.6 |

[a] Glass Transition temperature measured by DMTA, [b] 5 % weight loss temperature measured by TGA, [c] Residue weight at 700 °C in $N_2$, [d] Average mass molecular weight , [e] Polydispersity, [f] determined by elemental analysis.

(Table 2)

| Polymer Sample + SWCNT | $T_g$ (°C) [a] | | $T_{d5}$ (°C) [b] | Residue (%) [c] | S/C [d] | Storage modulus (GPa) | |
|---|---|---|---|---|---|---|---|
| | E'' | Tan δ | | | | at 100 °C | at 300 °C |
| - | 415 | 429 | 465 | 65 | 0.098-0.085 | 4.1 | 2.5 |
| 0.1 wt. % | 405 | 425 | 472 | 61 | 0.075 | 4.8 | 3.1 |
| 0.2 wt. % | 410 | 429 | 469 | 63 | 0.087 | 3.3 | 2.5 |
| 0.5 wt. % | 395 | 415 | 472 | 59 | 0.081 | 4.7 | 2.6 |
| 1 wt.% | 415 | 435 | 465 | 57 | 0.091 | 3.9 | 2.6 |
| 5 wt.% | 415 | 430 | 465 | 57 | 0.081 | 5.6 | 3.6 |
| 15 wt. % | 380 | 410 | 465 | 61 | 0.059 | 4.9 | 3.2 |

[a] Glass Transition temperature measured by DMTA, [b] 5 % weight loss temperature measured by TGA, [c] Residue weight at 700 °C in $N_2$, [d] determined by elemental analysis.

(Table 3)

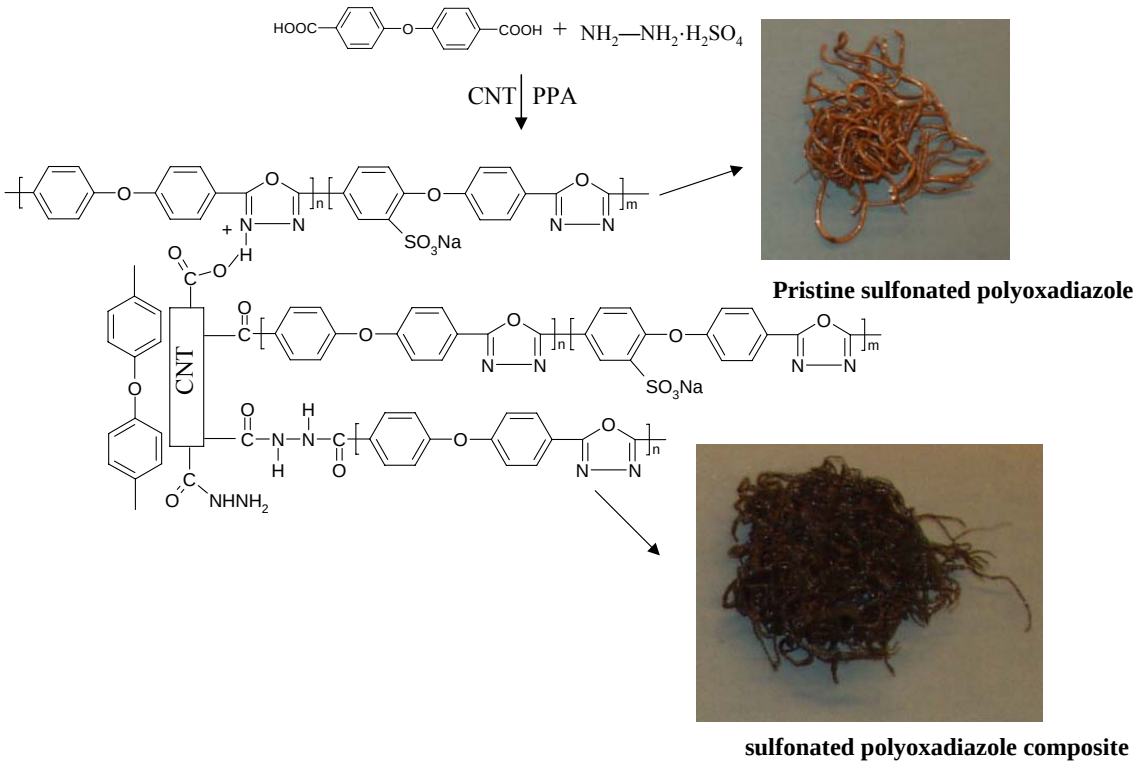
HOOC
COOH
+ NH2—NH2·H2SO4
CNT
PPA
SO3Na
CNT
NHNH2
Pristine sulfonated polyoxadiazole
sulfonated polyoxadiazole composite

(Figure 1)

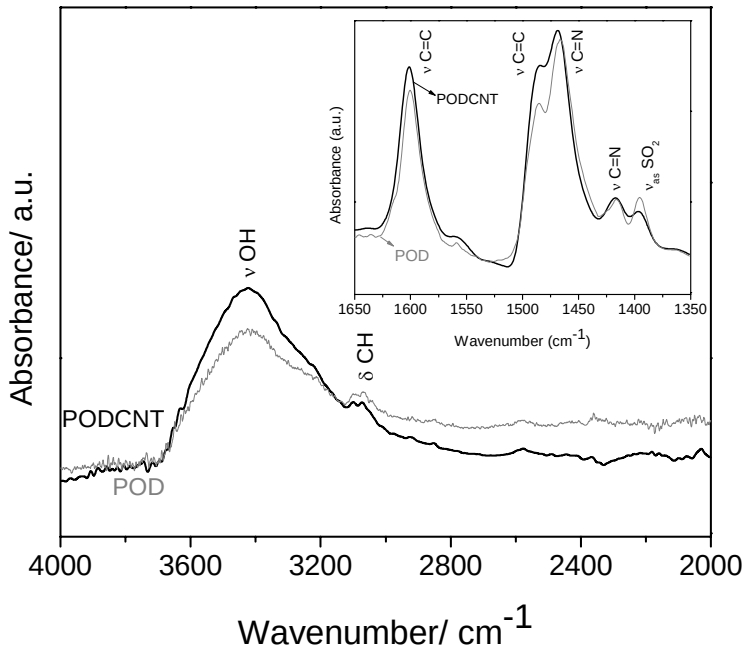
Absorbance/ a.u.
Wavenumber/ cm-1
4000
3600
3200
2800
2400
2000
PODCNT
POD
ν OH
δ CH
Absorbance (a.u.)
Wavenumber (cm-1)
1650
1600
1550
1500
1450
1400
1350
ν C=C
ν C=C
ν C=N
ν C=N
ν as SO2
PODCNT
POD

(Figure 2)

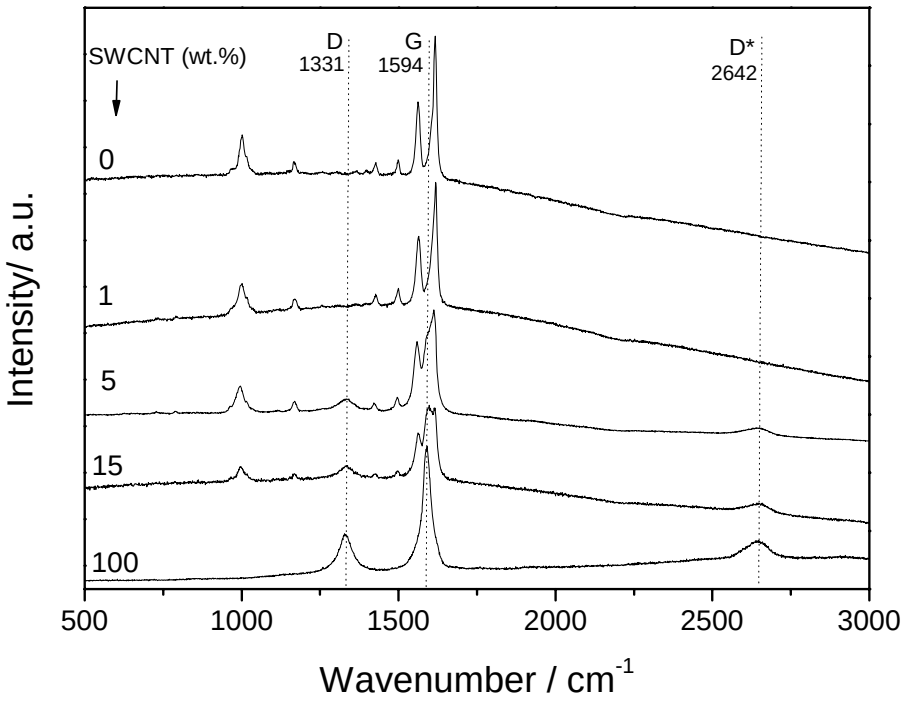
SWCNT (wt.%)
D
1331
G
1594
D*
2642
0
1
5
15
100
Intensity/ a.u.
500
1000
1500
2000
2500
3000
Wavenumber / cm-1

(Figure 3)

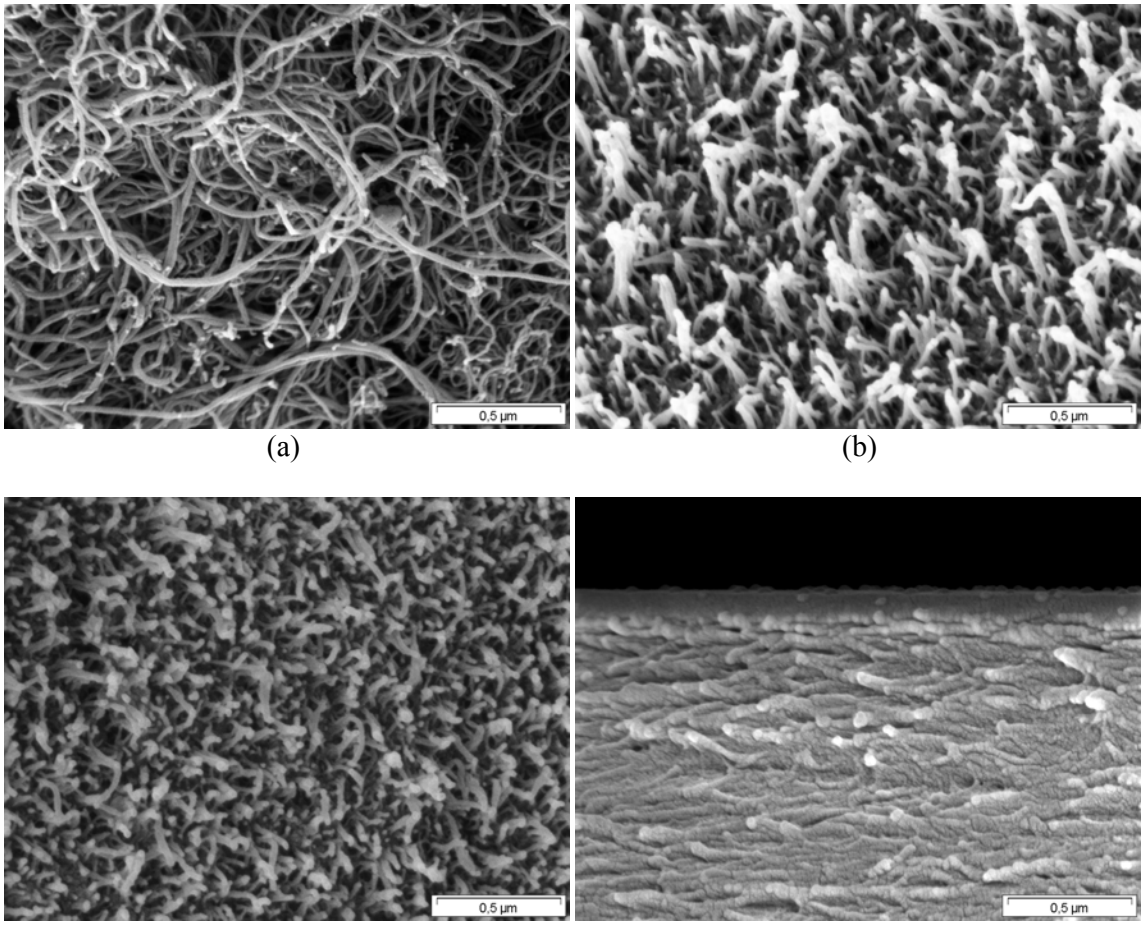


(a) (b)

(c) (d)

(Figure 4)

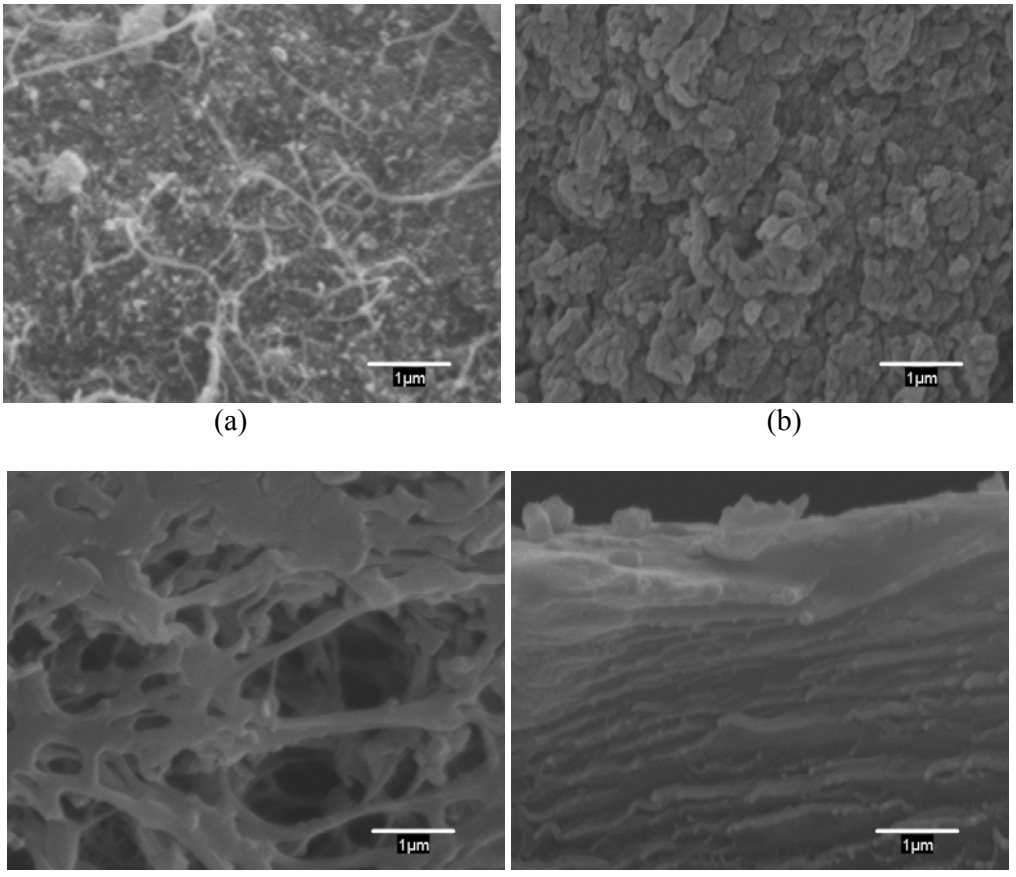


(a) (b)

(c) (d)

(Figure 5)

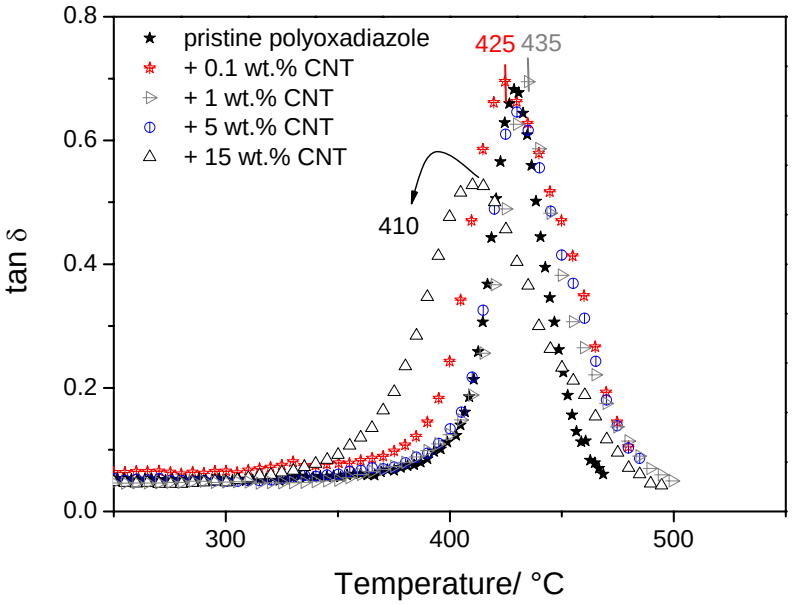
pristine polyoxadiazole
+ 0.1 wt.% CNT
+ 1 wt.% CNT
+ 5 wt.% CNT
+ 15 wt.% CNT
425
435
410
tan δ
Temperature/ °C
0.0
0.2
0.4
0.6
0.8
300
400
500

(Figure 6)

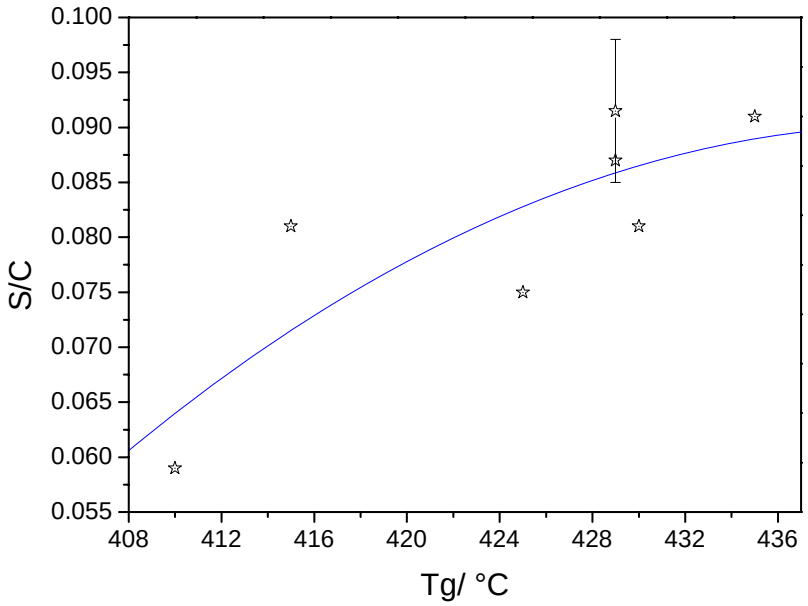
0.100
0.095
0.090
0.085
0.080
0.075
0.070
0.065
0.060
0.055
S/C
408
412
416
420
424
428
432
436
Tg/ °C

(Figure 7)

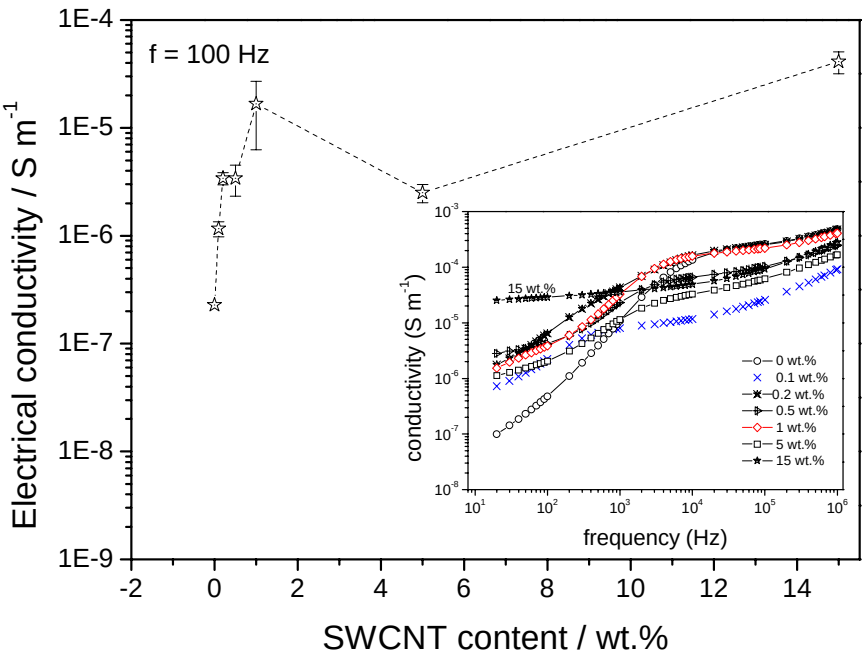
f = 100 Hz
Electrical conductivity / S m-1
SWCNT content / wt.%
1E-4
1E-5
1E-6
1E-7
1E-8
1E-9
-2
0
2
4
6
8
10
12
14
conductivity (S m-1)
frequency (Hz)
15 wt.%
0 wt.%
0.1 wt.%
0.2 wt.%
0.5 wt.%
1 wt.%
5 wt.%
15 wt.%

(Figure 8)